

SURFACE MODIFICATION AND MODULATION IN MICROSTRUCTURES: CONTROLLING PROTEIN ADSORPTION, MONOLAYER DESORPTION, AND MICRO-SELF-ASSEMBLY

Karl F. Böhringer

University of Washington, Department of Electrical Engineering
Seattle, WA 98198-2500, USA
E-mail: karl@ee.washington.edu

Abstract

The surface-to-volume ratio increases with decreasing scale, thus, controlling and changing the surface properties of microstructures can be a powerful tool in the design, fabrication, and use of microsystems. This paper overviews several recent projects that utilize the modulation of surfaces from hydrophobic to hydrophilic and vice versa, or from protein adsorbing to non-fouling, with applications in biomedical microdevices and self-assembling microelectromechanical systems (MEMS).

Key Words: surface modification, self-assembled monolayer, hydrophobic, hydrophilic, protein adsorption, bio-fouling, self-assembly, MEMS.

I. INTRODUCTION

Careful design and control of surface properties can be of great benefit in engineered microsystems. The laws of scaling entail that with decreasing size, effects tied to surface area (e.g., capillarity, electrostatic charge, adsorption of molecular layers) increasingly dominate effects tied to volume (e.g., gravity, inertia). This is the well-known cube-square-law, which relates the cubic scaling of volume to the quadratic scaling of surfaces; one of its consequences is the necessary existence of a “crossover point” where the surface effect starts to overtake the volume effect. This crossover point is typically seen at scales of just below 1mm [1].

Thus, a systematic study of surface properties at the microscale, combined with methods for controlling and modifying them, has been the topic of extensive recent research. In this paper, we investigate this field in greater detail, spanning a range of research activities from microelectromechanical “smart surfaces,” to micropatterned “programmable chemistry” that controls wettability and bio-fouling, to self-assembling microsystems.

The remainder of this paper is organized as follows: Section II begins with earlier work on “smart surfaces” comprising arrays of microactuators, which are employed for micropositioning tasks. Section III investigates assembly at the microscale, describing massively parallel approaches for self-assembly based on capillary forces. In Section IV, we discuss surface modifications to control hydrophobicity and protein adsorption, which has various applications in microassembly and biomedical microdevices. We conclude this paper with a summary and an outlook on open problems and future work.

II. CILIARY MICROSYSTEMS

During the past decade, several research groups have studied arrayed microactuators [2-22], obtaining their inspiration from biological cilia and distributed robotic conveyor systems. While these systems differ somewhat from the central theme of this paper (MEMS cilia are discrete mechanical devices, while here we want to focus on continuous properties of surfaces), there are still good reasons to review this earlier work: First, these systems represent a different kind of “smart surface” able to interact with objects in contact in a controlled, programmable fashion. Second, cilia arrays have given rise to a general theory of massively parallel, distributed manipulation [18], which is directly applicable to self-assembling systems. Here, we briefly review some of our work on microactuator arrays and summarize important theoretical results on micromanipulation and microassembly.

Actuator arrays built in single crystal silicon were introduced in the early 1990’s [7, 11]. Several thousand actuators were integrated in a dense layout on a single chip (Figure 1). These arrays were able to move small chiplets placed on top of them; however, the small range of motion (approximately 5 μ m) and limited force of each individual actuator rendered them less effective for general micromanipulation tasks.

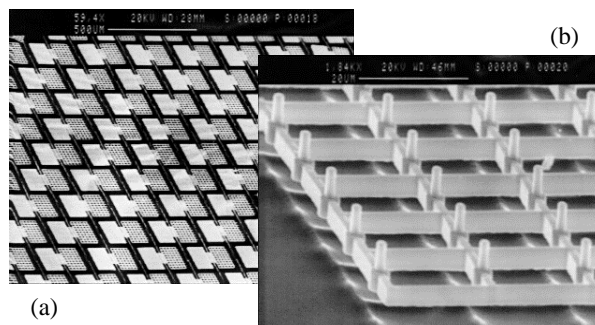


Figure 1: (a) Array of single crystal silicon microactuators. Individual actuator size is $240\mu\text{m} \times 180\mu\text{m}$. (b) Actuator detail with suspended silicon structures (spacing between posts: $20\mu\text{m}$). Figures from [11].

Suh *et al.* [15, 19] built several kinds of thermal bimorph polyimide microcilia, which were successfully used to position and orient millimeter-sized objects (Figure 2) under optical and scanning electron microscopes [18, 23]. Employed upside-down, these cilia arrays also enabled the first “walking” microrobot with full 3 degrees of freedom [24].

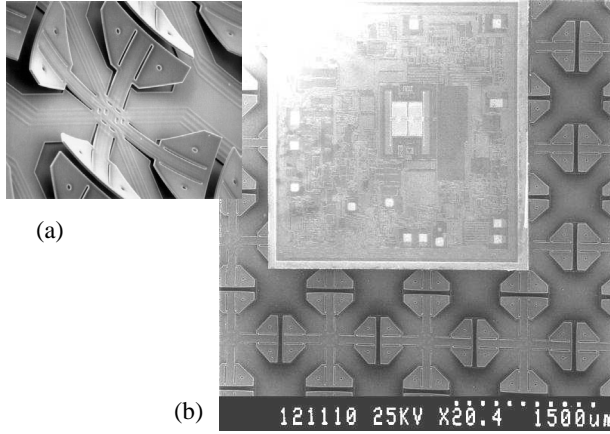


Figure 2: (a) “Motion pixel” made of 4 polyimide microcilia (total size 1.1mm × 1.1mm). (b) Cilia array transporting an ADXL50 chip (size about 3mm × 3mm). Figures from [15] by J. Suh.

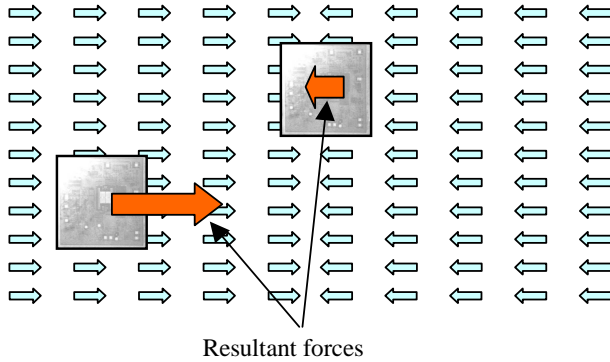


Figure 3: Concept of a programmable force field (PFF) for positioning of microparts. The force acting on the part is obtained by integrating the PFF over its surface area. A microactuator array could be used to generate this PFF.

Coordinating hundreds or thousands of individual cilia to achieve a micropositioning task has been the topic of extensive research in robotics [18, 25, 26], which is beyond the scope of this paper. Here, we simply present some key findings that will be useful in our further discussion.

Modeling of microactuator arrays is conveniently accomplished with force vector fields, which assign a lateral force to each point in the plane. For example, Figure 3 shows such a force vector field and its effect on two objects that are placed on top of it.

Even simple fields consisting only of two separate regions with constant force vectors are sufficient to position an object without any sensor feedback. Figure 3 shows the underlying principle: The lateral force on an object in contact integrates over its contact area. The resultant force for the left part is a larger force pointing towards the right. The resultant force for the right part, however, is a smaller force towards the left, since its contact area encompasses regions of forces pointing to the left as well as to the right. It is easy to see that there exist placements where the part is in equilib-

rium. These equilibria are the final rest positions for an object that is placed at an arbitrary initial position.

We can thus think of microactuator arrays as “programmable force fields” (PFF’s). It has been shown that PFF’s can efficiently perform a broad range of micromanipulation tasks such as positioning, orienting, and sorting [18, 25]. In addition, these general results on PFF’s are very useful to devise strategies for massively parallel microassembly. The next section will investigate microassembly in greater detail.

III. MICRO-SELF-ASSEMBLY

Recent developments in the area of microfabrication techniques offer the opportunity to create a large variety of functional microdevices (*e.g.*, chemical, electrical, mechanical, and optical transducers). Practical applications require integration of such devices into compact and robust microsystems. Monolithic integration often faces problems of material and process incompatibilities of different functionalities. Ideally, one would like to build each functional subsystem with optimized materials and processes, and then assemble them into a complex microsystem. Researchers have been investigating the adoption of macroscale “pick and place” methods to assemble micro- or even nanoscale components [27-29]. One major concern in these approaches is the “sticking effect” between assembly manipulators and components, due to electrostatic, van der Waals, or surface tension forces [1]. On the other hand, new assembly approaches have emerged by taking advantage of this sticking effect: Whitesides and co-workers first demonstrated capillary-force-driven assembly of a simple circuit [30]; Srinivasan *et al.* extended the capillary-force-driven strategy to assemble identical microscopic parts onto a single substrate [31]. In this section, we describe a novel approach based on capillary action to achieve multiple batch assembly and bonding of microcomponents onto a substrate. In addition, electroplating as a post assembly process is used to establish electrical connections for assembled components in a parallel manner [32-35].

III.1 SELF-ASSEMBLY PRINCIPLES

In our assembly method, capillary force is exploited to drive the assembly, and the force is created by a hydrocarbon-based lubricant between hydrophobic surfaces as in [30, 31]. A schematic illustration of our assembly process is shown in Figure 4. We fabricate a silicon substrate with gold patterns as destined binding sites for assembly of parts (Figure 4a). To activate the binding sites on the substrate, a hydrophobic alkanethiol ($\text{CH}_3(\text{CH}_2)_n\text{SH}$) self-assembled monolayer (SAM) is adsorbed on hydrophilic gold patterns. For each batch of microparts, only desired binding sites on the substrate are activated by selectively de-activating other binding sites. In the de-activation process, electrochemical reductive desorption of the SAM, *i.e.*, $\text{CH}_3(\text{CH}_2)_n\text{SAu} + e^- \rightarrow \text{Au} + \text{CH}_3(\text{CH}_2)_n\text{S}^-$ [36, 37] is performed (Figure 4b). Thus we can control the assembly not to occur in the gold regions where the SAM desorption has taken place. To create the driving force, we apply a lubricant to the substrate prior to assembly. Next, the substrate is immersed in water and the lubricant forms droplets exclusively on the activated binding sites. After the parts are transferred into water, the parts with a hydrophobic side are attracted and aligned to the binding sites on the substrate.

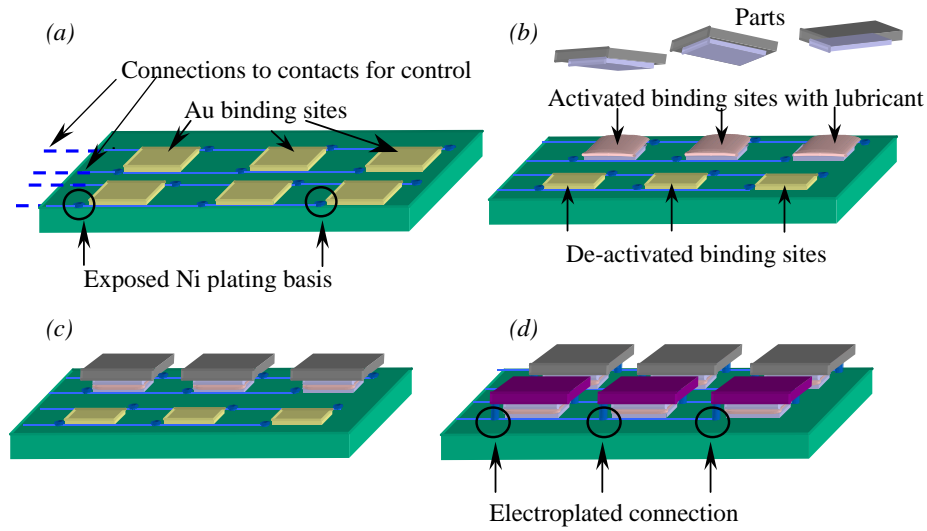


Figure 4: Schematic flow of multi-batch capillary-force-driven self-assembly. (a) A fabricated substrate for assembly with gold binding sites and nickel plating basis. (b) A substrate prepared for first batch assembly. The substrate is immersed in water with lubricant wetting exclusively the activated binding sites. (c) First batch assembly. (d) By repeating the assembly process, the second batch of components is assembled. Electroplating is performed afterwards to establish electrical connections. Figure from [35] by X. Xiong.

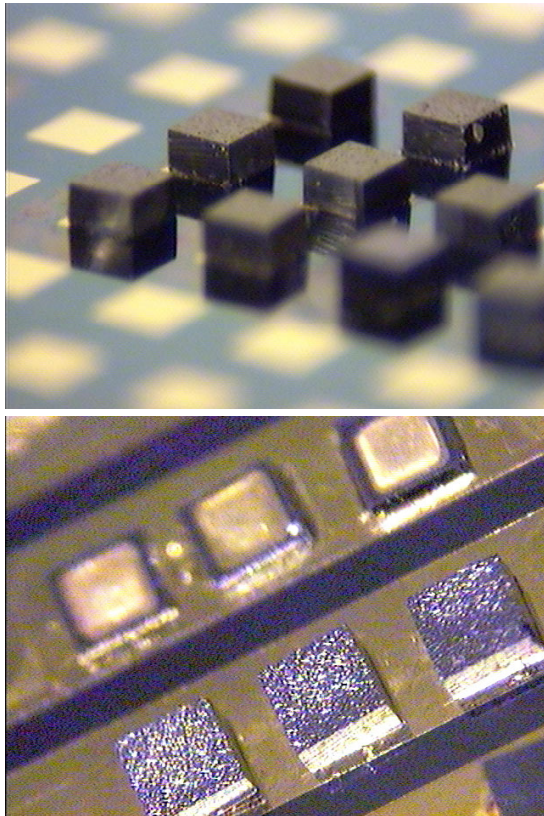


Figure 5: Assembly results. (a) An assembly result of one batch diced silicon chips. (b) A two-batch assembly result. Figure from [32,33] by Y. Hanein and X. Xiong.

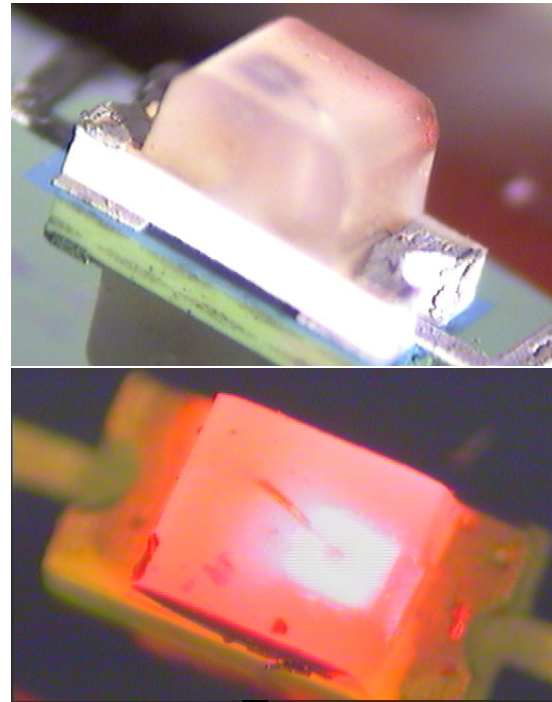


Figure 6: (a) An assembled LED. (b) An assembled LED with electrical connections to the substrate. The LED is activated by applying potential bias to the contacts on the substrate. Figures by X. Xiong.

The lubricant can be cured by heat and permanently bonds the part to the substrate (Figure 4c). The SAM adsorption, desorption and assembly steps can be repeated for multiple batches of parts assembly. Finally, electrical connections can be established between the assembled parts and the substrate by electroplating (Figure 4d).

III.2 EXPERIMENTS AND RESULTS

To demonstrate the assembly, we use two different kinds of components: silicon diced chips ($1\text{mm} \times 1\text{mm}$) with one gold-coated side and commercial light emitting diodes (LED's). Destined substrates for assembly are specifically designed for different kinds of components. For the square silicon chips, electrically isolated gold stripes are patterned in a lift-off process on a silicon substrate with a thermal oxide layer of approximately 4000\AA . A passivation layer of silicon nitride is patterned by photolithography and reactive ion etching (RIE) until gold squares ($1\text{mm} \times 1\text{mm}$) as the binding sites are exposed. The substrate for LED assembly has an additional metallization layer of 350\AA Cr/Ni, which is patterned as the basis for electroplating prior to the Cr/Au layer deposition. To activate the binding sites for assembly, a SAM is adsorbed on all the gold binding sites after immersed in ethanolic dodecanethiol solution for several hours. For multi-batch assembly, desired binding sites for the first batch assembly remain hydrophobic, while other binding sites are de-activated and transformed to hydrophilic via an electrochemical SAM desorption process [32].

To prepare for the assembly, a hydrocarbon lubricant composed of 97wt.% triethyleneglycol dimethacrylate (Sigma) as crosslinker, and 3wt.% benzoyl peroxide (Sigma) as thermal initiator is spread on the whole substrate. The substrate is then immersed in water. The lubricant wets only the activated binding sites in water. When parts with hydrophobic binding sites are added in water, the parts are attracted and self-aligned to the binding sites on the substrate simultaneously. The lubricant is then polymerized by heating the substrate at 80°C for thirty minutes, which permanently bonds the parts to the substrate. Figure 5a shows assembly results from one batch of silicon test chips. A second assembly is performed by repeating SAM formation and the assembly steps. A two-batch assembly is demonstrated in Figure 5b. After the assembly, electrical connections between the parts and the substrate are established by electroplating. We use LED's to demonstrate both assembly and electroplating methods. Figure 6a is an example of an assembled LED. Figure 6b is an assembled LED with electrical connection to the substrate, and the LED is activated by potential bias applied on the contacts on the substrate.

III.3 BINDING SITE DESIGN

Binding site design is important for assembly, since optimal binding site design can provide for higher alignment accuracy, higher assembly yield, shorter assembly time, and uniqueness of assembly orientation. When using commercial off-the-shelf parts such as LED's with given design as shown in Figure 7a, a straightforward binding site design would simply use the same pattern as the part. However, it was shown that such a design will not always be optimal and misalignment may occur in assembly [38]. To improve as-

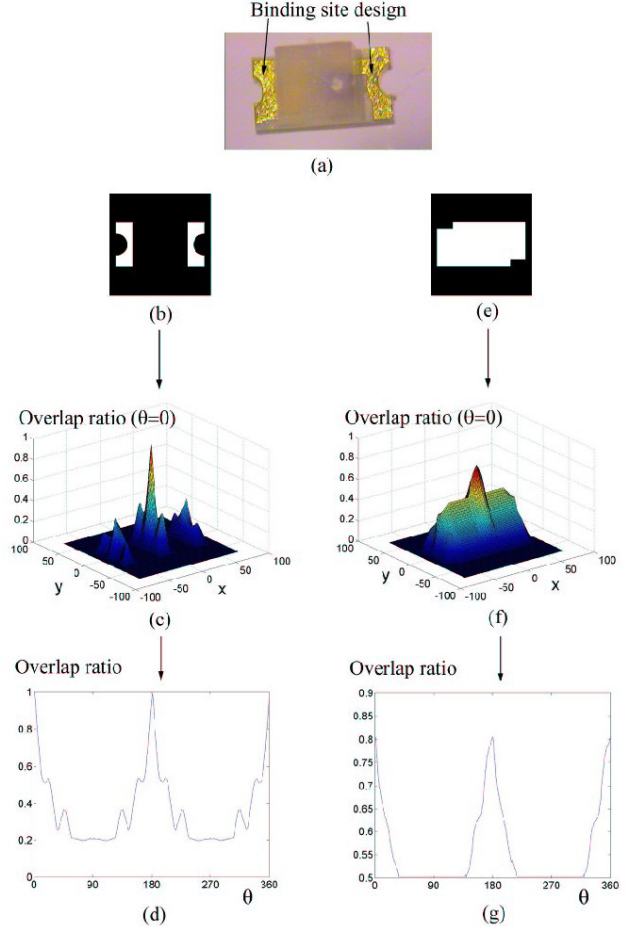


Figure 7: (a) A commercial LED with given binding site design. (b) An intuitive design for the substrate binding site is the same as the binding site pattern of the LED. (c) Translation and (d) rotation simulations for the design in (b). (e) Another binding pattern design for LED assembly, with the openings on the top-left and bottom-right corners for placing the electroplating bases. (f) Translation and (g) rotation simulations for the design shown in (e). Figures by X. Xiong.

sembly, we custom design the binding site and plating basis geometry using a software simulation tool [33, 38].

The simulation tool is based on a simple surface energy model of our self-assembly system. It uses the observation that self-assembly and self-alignment is the result of minimization of interfacial energy between the lubricant meniscus and the aqueous environment. As described in [33, 38], the interfacial energy is directly proportional to the exposed hydrophobic surfaces in water. In a first-order approximation, the surface energy W can be represented in terms of the hydrophobic regions on the part and the substrate, denoted by P and S respectively, as long as the lubricant bridge height is small compared to the binding site length or width:

$$W = \gamma (|S| + |P| - 2 |S \cap P|) \quad (1)$$

Here γ is the interfacial energy coefficient, and $|S|$ and $|P|$ denote the surface area of a region S and P , respectively.

Since the terms $|S|$ and $|P|$ in Eq. 1 are constants, W is directly proportional to $-|S \cap P|$: the negated overlap area between S and P . A concise and rigorous derivation of this model is presented in [33].

It is worth noting that the gradient of the surface energy, ∇W , represents a vector field that provides the driving force for the self-assembly process. Thus, the results obtained for programmable force fields (PPF's) as summarized in Section II can be applied here. This is particularly interesting since ∇W can be modulated during the assembly process with the desorption of hydrophobic SAM's.

To briefly describe the implementation of the simulation tool, the overlap area called $A(x,y,\theta)$ is computed with respect to three parameters, representing the relative location (x,y) and orientation θ of P to S . For a given orientation θ , the value A can be calculated efficiently by two-dimensional convolution of P to S . To characterize the overlap area as a function of rotation angle, calculations are iterated for discretized θ values in the range from 0° to 360° .

Therefore, for a binding site design, we use two plots to show the simulation results: translation and rotation. In the translation result, the overlap ratio, which is the ratio of the overlap area to part binding site area $|S \cap P| / |P|$ is plotted as a function of relative location (x,y) of P to S . In the rotation result, each point in the plot corresponds to a maximum overlap ratio with respect to a given orientation θ .

Ideally, assembly configurations should possess a unique global energy minimum, which, according to our model, would correspond to a unique maximum of area overlap as a function of (x,y,θ) . With the given symmetric LED binding site design shown in Figure 7a, such a unique maximum is impossible to achieve. Figures 7b and 7e show two different binding site designs, and the design in Figure 7b is simply a copy of the LED binding site design. Figures 7c and 7d are the translation and rotation simulation results for design (b), and Figures 4f and 4g are the simulation results for design (e). Figure 4b shows multiple local maxima for binding site design (b) at 0° , while Figure 4e shows only one maximum for design (e). Figures 4c and 4f show that design (b) has multiple maxima at various orientations, while design (e) has only two maxima for 0° and 180° (there must be two maxima because the LED design is symmetric). These simu-

lation results indicate that design (d) is preferable, as it exhibits only two maxima in overlap.

III.4 DISCUSSION

In this section, we have presented a self-assembly protocol as well as a modeling tool for design and simulation of capillary-force-driven self-assembly. Parallel self-assembly has been demonstrated with multiple batches of different microparts, and also with commercial-off-the-shelf LED's. As an enabling technology, this approach offers the prospect of efficient integration of complex microsystems from a range of different microcomponents. Currently, we are applying this approach to construct hybrid complex systems such as microfluidic devices. By expanding and modifying the current assembly processes, we are able to assemble the piezoelectric actuating elements with precise placement and establish electrical connections through post-bonding electroplating in order to construct hybrid piezoelectric micropumps.

With the emergence of more and more diverse processes, materials, and devices for microsystems, we believe micro-self-assembly will be a key technique for system integration. The self-assembly protocol demonstrated in this section provides a feasible solution to overcome the incompatibility between system components and helps to achieve optimal materials and designs for individual components. It is anticipated that this technique can be applied to a wide range of components for the integration and packaging of complex systems.

Furthermore, this technique motivates us to investigate surface-force-driven self-assembly in more general terms. Exploiting the hydrophobic effect of SAM's in an aqueous solution is just one of many possible approaches. In the following section, we present another technique to modify surface properties at the microscale, by integrating a "smart polymer" into MEMS processes. This provides not only a method for controlling hydrophobicity simply with an electrical signal, but it can be used to steer the adsorption of proteins and cells on micropatterned surfaces.

IV. PROGRAMMABLE SURFACES WITH "SMART POLYMERS"

Surface chemistry can be exploited to control a wide range of phenomena such as hydrophobicity and bio-fouling, *i.e.*,

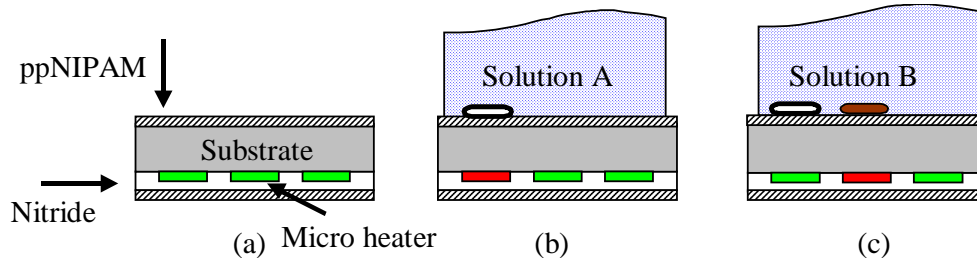


Figure 8: Schematic description of ppNIPAM devices. (a) Devices consist of micro-heaters on a glass slide coated with ppNIPAM. (b) Active heater (dark) turns the surface hydrophobic and fouling. Selective protein adsorption occurs exclusively on heated areas. Protein adsorption takes place on the top side of the substrate. (c) A second adsorption step with different protein solution on a different heater. Figure from [43] by Y. Wang.

the tendency of biological substances (proteins, cells, biofilms, *etc.*) to attach to exposed surfaces. Over the past decades, a wide range of materials have been developed and studied, such as poly(ethylene glycol) or poly(ethylene oxide) (PEG's, PEO's) [39, 40] especially for applications in biomedical devices and implants. Poly-N-isopropylacrylamide (pNIPAM) is another particularly interesting candidate polymer material to realize programmable surface chemistry. Among its properties is a transition from hydrophilic and non-fouling behavior at room temperature to hydrophobic and fouling behavior above its lower critical solution temperature (LCST). In addition, its LCST of 32°C is close to body temperature and thus suitable for protein treatment. These properties are due to the reversible formation and cleavage of the hydrogen bonds between NH or C=O groups and surrounding water molecules with changing temperature [41].

A plasma polymerized form of pNIPAM (ppNIPAM) has been developed at the University of Washington that demonstrates the same favorable properties as the bulk material [42]. In this section, we show how vapor-phase deposited ppNIPAM on microfabricated heater arrays opens the door for controlling the surface chemistry at the microscale.

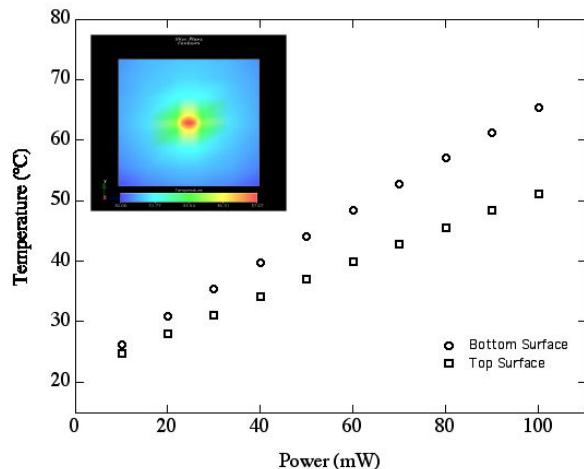


Figure 9. Simulated center temperature of top and bottom surfaces versus power (using CoventorTM). Inset: Temperature profile of the top surface for 50mW. Data from actual devices agrees with values predicted for the bottom surface temperature. Figure from [43] by A. Shastry and Y. Wang.

IV.1 EXPERIMENTAL SETUP

In this section we present a recently developed method to pattern proteins using programmable surfaces consisting of ppNIPAM [43]. Figure 8 shows the principles of our method.

The microfabrication process consists of CrAuCr heaters (thickness 150nm, area 1mm × 0.8mm, and 40µm wide lines) deposited on a glass substrate (thickness 180µm). The heaters are passivated with sputtered silicon nitride (400nm) and the entire device is then treated with ppNIPAM in a plasma deposition process [42]. This process is particularly suited

for MEMS applications as it ensures very high surface coverage, excellent adhesion and good non-fouling properties at room temperature [44]. CoventorTM, a fully integrated finite element simulation package, is used to simulate the electrothermal properties of the designed heaters (Figure 9). Temperature sensitive paint is used to characterize the heating profile.

When exposed to protein solution, proteins are adsorbed exclusively at heated areas. These protein patches remain immobilized even after the heater is turned off and the temperature is dropped below the LCST. Repeated adsorption steps form arrays of protein patches such as those required for protein chips.

IV.2 EXPERIMENTAL RESULTS

A fabricated microheater array is shown in Figure 10a. Immunoglobulin G (IgG) test results are shown in Figure 10b and 10c. The microheater chip was first incubated with fluorescein isothiocyanate (FITC)-anti-BSA for 30 minutes with the upper heater turned on (94mW). The heater was then turned off and the chip was incubated with tetramethylrhodamine isothiocyanate (TRITC)-goat-IgG with the middle heater turned on for another 30 minutes. The two fluorescence images (Figures 10b and 10c) were taken from the same chip at two different wavelengths. Two patches of proteins can be clearly identified on the device surface. The second protein batch did not adhere to areas already covered with anti-BSA.

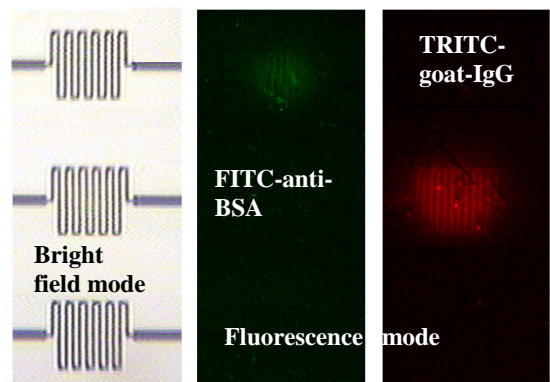


Figure 10: (a) Micro-heater array: 3 resistive CrAuCr heaters, thickness 150nm, linewidth 40µm, area approximately 1mm². (b) FITC-anti-BSA pattern adsorbed on top heater. (c) TRITC-goat-IgG pattern adsorbed on center heater. All figures are taken from the same substrate at different wavelengths, after the two protein adsorptions. Figures from [43] by X. Cheng and Y. Wang.

IV.3 DISCUSSION

The technique described in this section offers a new approach to realize programmable surface chemistry devices by using microheater arrays to control the properties of a ppNIPAM coating. Controlled protein adsorption in several batches has been demonstrated, and could be applied to create larger arrays for protein chips. The performance of these de-

vices with multiple proteins, with cells and for additional MEMS and bioMEMS applications are currently being investigated.

A major advantage of the presented technique is the ability to perform the entire process in a wet environment, which is critical to maintain the integrity of sensitive proteins during the patterning processes. Additional major advantages are the simple setup and the low power consumption.

In addition to the fouling/non-fouling change, ppNIPAM also exhibits a hydrophobic/hydrophilic change in aqueous environment in response to relatively small changes in temperature, which suggests many other uses. In particular, we believe that a combination of the micro-self-assembly techniques described in Section III and programmable ppNIPAM surface chemistry of this section can produce a new generation of self-assembling systems that takes advantage of this simple technique for programmable surface chemistry.

V. CONCLUSIONS

This paper has overviewed several projects on microfabricated devices by attempting to show a common theme: that the control of surface properties is of central importance in the design and use of microdevices. Various techniques already exist to tune and program surfaces at the microscale: by actuation with ciliary microarrays, by electrochemical modulation of hydrophobicity and the deliberate use of capillary forces, or by integration of temperature-responsive polymers into MEMS devices. However, these are just a few of the many possibilities that open up in this rapidly expanding field. While various groups have reported initial successes, many questions remain; here, we list just a few fundamental ones:

- We now know that surface effects dominate volume effects at the microscale, and that this can be exploited to create novel devices and manufacturing techniques that would not be possible at larger scales. However, as we scale further down towards nanometer dimensions, will the laws of scaling continue to work in our favor? For example, the capillary-force-driven self-assembly may only work well as long as the micropart is significantly larger than the lubricant droplet. Otherwise, good alignment can no longer be expected. Thus, nanoscale parts may self-assemble better by exploiting closer range interactions such as van der Waals forces or recombinant nucleotides.
- What are the fundamental principles that describe and limit self-assembly? Recent work has shown an intricate relationship between assembly yield and alignment accuracy not only with surface chemistry, but also with three-dimensional part design, binding site density, and the specifics of part delivery. What is needed is a comprehensive model for the dynamics of micro-self-assembly.

ACKNOWLEDGEMENTS

The work in this paper represents numerous collaborations for which I am immeasurably grateful. The following list of

collaborators must remain incomplete, but special thanks go to the following people: Bruce R. Donald, Noel MacDonald, and Rob Mihailovich for their work on single crystal silicon actuator arrays and on programmable force fields; Bruce Darling, Bruce R. Donald, Greg Kovacs, and John Suh on MEMS cilia; Jiandong Fang, Yael Hanein, Daniel Schwartz, Weihua Wang, and Xiaorong Xiong for the SAM-driven micro-self-assembly; and Xuanhong Cheng, Denice Denton, Yael Hanein, Buddy Ratner, Ashutosh Shastry, and Yanbing Wang for the work with ppNIPAM.

We would like to thank Roger T. Howe, Uthara Srinivasan, and Mike Sinclair for inspiring discussions and Michael B. Cohn for providing microparts.

Fabrication of the single crystal silicon actuator arrays was performed at the Cornell Nanofabrication Facility. The MEMS polyimide cilia were built at the Stanford Nanofabrication Facility. Samples for the electrochemically controlled self-assembly and the ppNIPAM microheaters were prepared at the University of Washington (UW) MEMS Laboratory, the UW Electrical Engineering Microfabrication Laboratory, the UW Bioengineered Materials Center, and the Washington Technology Center. We thank the staff and users of these institutions for their help and support.

This research was supported in part by NSF awards ECS-0223598, EIA-0072744, and ECS9875367 (CAREER award to K. Böhringer), NIH award *CEGSTech: Biologically Active Microsystems*, Packard Foundation grant 2000-01763, DARPA Bio:Info:Micro grant MD A972-01-1-0002, Washington Technology Center MEMS awards 99-A and 99-8, a Ford Fellowship to X. Xiong, as well as donations from Agilent Technologies, Intel Corporation, Microsoft Research, Tanner Research Inc. and Technic Inc.

REFERENCES

- [1] Fearing, R.S., Survey of Sticking Effects for Micro Parts Handling, in *IROS - IEEE/RSJ International Workshop on Intelligent Robots & Systems*. 1995. Pittsburgh, PA.
- [2] Pister, K.S.J., R. Fearing, and R. Howe, A planar air levitated electrostatic actuator system, in *Proc. IEEE 5th Workshop on Micro Electro Mechanical Systems*. 1990. Napa Valley, CA.
- [3] Furihata, T., T. Hirano, and H. Fujita, Array-driven ultrasonic microactuators, in *Transducers '91 Dig. 6th Int. Conf. on Solid State Sensors and Actuators*. 1991. San Francisco, CA.
- [4] Takeshima, N. and H. Fujita, Polyimide bimorph actuators for a ciliary motion system, in *ASME WAM, Symp. Micromech. Sensors, Actuators, and Systems*. 1991.
- [5] Fujita, H., Group Work of Microactuators, in *International Advanced Robot Program Workshop on Micro-machine Technologies and Systems*. 1993. Tokyo, Japan.
- [6] Ataka, M., A. Omodaka, and H. Fujita, A biomimetic micro motion system, in *Transducers '93 Dig. 7th Int. Conf. on Solid State Sensors and Actuators*. 1993. Pacifico, Yokohama, Japan.
- [7] Böhringer, K.F., B.R. Donald, R. Mihailovich, and N.C. MacDonald, A Theory of Manipulation and Control for Microfabricated Actuator Arrays, in *IEEE Workshop on*

- Micro Electro Mechanical Systems (MEMS)*. 1994. Oiso, Japan.
- [8] Konishi, S. and H. Fujita, A conveyance system using air flow based on the concept of distributed micro motion systems, *Journal of Microelectromechanical Systems*, 1994. **3**(2): p. 54-58.
- [9] Liu, C., T. Tsai, Y.-C. Tai, W. Liu, P. Will, and C.-M. Ho, A micromachined permalloy magnetic actuator array for micro robotics assembly systems, in *Transducers '95 Dig. 8th Int. Conf. on Solid-State Sensors and Actuators/Eurosensors IX*. 1995. Stockholm, Sweden.
- [10] Liu, W. and P. Will, Parts manipulation on an intelligent motion surface, in *IEEE/RSJ Int. Conf. on Intelligent Robots and Systems*. 1995. Pittsburg, PA.
- [11] Böhringer, K.-F., B.R. Donald, and N.C. MacDonald, Single-crystal silicon actuator arrays for micro manipulation tasks, in *Proc. IEEE 9th Workshop on Micro Electro Mechanical Systems (MEMS)*. 1996. San Diego, CA.
- [12] Suh, J.W., S.F. Glander, R.B. Darling, C.W. Storment, and G.T.A. Kovacs, Combined organic thermal and electrostatic omnidirectional ciliary microactuator array for object positioning and inspection, in *Solid-State Sensors and Actuator Workshop*. 1996. Hilton Head, SC.
- [13] Nakazawa, H., Y. Watanabe, and O. Morita, The two-dimensional micro conveyor: Principles and fabrication process of the actuator, in *Transducers '97 Dig. 9th Int. Conf. on Solid-State Sensors and Actuators*. 1997. Chicago, IL.
- [14] Mita, Y., S. Konishi, and H. Fujita, Two dimensional micro conveyance system with through holes for electrical and fluidic interconnection, in *Transducers '97 Dig. 9th Int. Conf. on Solid-State Sensors and Actuators*. 1997. Chicago, IL.
- [15] Suh, J.W., S.F. Glander, R.B. Darling, C.W. Storment, and G.T.A. Kovacs, Organic thermal and electrostatic ciliary microactuator array for object manipulation, *Sensors and Actuators, A: Physical*, 1997. **58**: p. 51-60.
- [16] Kladitis, P.E., V.M. Bright, K.F. Harsh, and Y.C. Lee, Prototype microrobotics for micro positioning in a manufacturing process and micro unmanned vehicles, in *IEEE 12th Workshop on Micro Electro Mechanical Systems (MEMS)*. 1999. Orlando, FL.
- [17] Böhringer, K.F., J.W. Suh, B.R. Donald, and G.T.A. Kovacs, Vector fields for task-level distributed manipulation: experiments with organic micro actuator arrays, in *IEEE International Conference on Robotics and Automation*. 1997.
- [18] Böhringer, K.F., B.R. Donald, and N.C. MacDonald, Programmable Vector Fields for Distributed Manipulation, with Applications to MEMS Actuator Arrays and Vibratory Parts Feeders, *International Journal of Robotics Research*, 1999. **18**(2): p. 168-200.
- [19] Suh, J.W., R.B. Darling, K.F. Böhringer, B.R. Donald, H. Baltes, and G.T.A. Kovacs, CMOS Integrated Organic Ciliary Array as a General-Purpose Micromanipulation Tool for Small Objects, *Journal of Microelectromechanical Systems*, 1999. **8**(4): p. 483-496.
- [20] Mita, Y., A. Kaiser, B. Stefanelli, P. Garda, M. Milgram, and H. Fujita, A distributed microactuator conveyance system with integrated controller, in *IEEE SMC*. 1999.
- [21] Ebefors, T., J.U. Mattsson, E. Kèlvesten, and G. Stemme, A robust micro conveyor realized by arrayed polyimide joint actuators, in *IEEE 12th Workshop on Micro Electro Mechanical Systems (MEMS)*. 1999. Orlando, FL.
- [22] Böhringer, K.F. and H. Choset, eds. *Distributed Manipulation*. 2000. Kluwer Academic Publishers. 272 pages.
- [23] Darling, R.B., J.W. Suh, and G.T.A. Kovacs, Ciliary Microactuator Array for Scanning Electron Microscope Positioning Stage, *Vacuum Science & Technology A*, 1998. **16**(3): p. 1998-2002.
- [24] Mohebbi, M.H., M.L. Terry, K.F. Böhringer, J.W. Suh, and G.T.A. Kovacs, Omnidirectional Walking Microrobot Using MEMS Thermal Cilia Arrays, in *ASME International Mechanical Engineering Congress and Exposition (IMECE'01)*. 2001. New York, NY.
- [25] Böhringer, K.F., B.R. Donald, L. Kavraki, and F. Lamiroux, Part Orientation with One or Two Stable Equilibria Using Programmable Vector Fields, *IEEE Transactions on Robotics and Automation*, 2000. **16**(2): p. 157-170.
- [26] Luntz, J.E., W. Messner, and H. Choset, Discreteness Issue in Actuator Arrays, in *Distributed Manipulation*, K.F. Böhringer and H. Choset, Editors. 2000. Kluwer Academic Publishers Group: Norwell, MA. p. 103-126.
- [27] Ralis, S.J., B. Vikramaditya, and B.J. Nelson, Micropositioning of a weakly calibrated microassembly system using coarse-to-fine visual servoing strategies, *IEEE Trans. on Electr. Packaging Manufacturing*, 2000. **23**(2): p. 123-131.
- [28] Yang, G., J.A. Gaines, and B.J. Nelson, A flexible experimental workcell for efficient and reliable wafer-level 3D micro-assembly, in *IEEE Int. Conference on Robotics and Automation (ICRA)*. 2001. Seoul, South Korea.
- [29] Thompson, J.A. and R.S. Fearing, Automating microassembly with ortho-tweezers and force sensing, in *IEEE/RSJ International Conference on Intelligent Robots and Systems (IROS)*. 2001. Maui, HI.
- [30] Terfort, A., N. Bowden, and G.M. Whitesides, Three-dimensional Self-Assembly of Millimetre-Scale Components, *Nature*, 1997. **386**: p. 162-164.
- [31] Srinivasan, U., R.T. Howe, and D. Liepmann, Microstructure to Substrate Self-Assembly Using Capillary Forces, *ASME/IEEE Journal of Microelectromechanical Systems*, 2001.
- [32] Xiong, X., Y. Hanein, W. Wang, D.T. Schwartz, and K.F. Böhringer, Controlled Part-To-Substrate Micro-Assembly Via Electrochemical Modulation of Surface Energy, in *Transducers'01 - International Conference on Solid-State Sensors and Actuators*. 2001. Munich, Germany.
- [33] Xiong, X., Y. Hanein, W. Wang, D.T. Schwartz, and K.F. Böhringer, Multi-Batch Micro-Selfassembly via Controlled Capillary Forces, in *IEEE/RSJ IROS 2001 - International Conference on Intelligent Robots and Systems*. 2001. Maui, HI.
- [34] Xiong, X., Y. Hanein, J. Fang, Y. Wang, W. Wang, D.T. Schwartz, and K.F. Böhringer, Controlled Multi-Batch

- Self-Assembly of Micro Devices, *Journal of Microelectromechanical Systems*, 2002: Submitted for review.
- [35] Xiong, X., Y. Hanein, J. Fang, D.T. Schwartz, and K.F. Böhringer, Multi-batch Self-assembly for Microsystem Integration, in *3rd International Workshop on Microfactories (IWMF'02)*. 2002. Minneapolis, MN.
- [36] Abbot, N.L., C.B. Gorman, and G.M. Whitesides, Active Control of Wetting Using Applied Electrical Potentials and Self-Assembled Monolayers, *Langmuir*, 1995. **11**: p. 16-18.
- [37] Walczak, M.M., D.D. Popenoe, R.S. Deinhammer, B.D. Lamp, C. Chung, and M.D. Porter, Reductive Desorption of Alkanethiolate Monolayers at Gold: A Measure of Surface Coverage, *Langmuir*, 1991. **7**(11): p. 2687-2693.
- [38] Böhringer, K.F., U. Srinivasan, and R.T. Howe, Modeling of Capillary Forces and Binding Sites for Fluidic Self-Assembly, in *IEEE MEMS'01 - International Conference on Micro Electro Mechanical Systems*. 2001. Interlaken, Switzerland.
- [39] Graham, N.B., N.E. Nwachuku, and D.J. Walch, Interaction of poly(ethylene oxide) with solvents: 1. Preparation and swelling of a crosslinked poly(ethylene oxide) hydrogel, *Polymer*, 1982. **23**: p. 1345-1349.
- [40] Andrade, J.D., V. Hlady, and S.-I. Jeon, Poly(ethylene oxide) and protein resistance in hydrophilic polymers - performance with environmental acceptance, *Advances in Chemistry*, 1996. **248**.
- [41] Heskins, M. and J.E. Guillet, Solution properties of poly(N-isopropylacrylamide), *J. Macromol. Sci. Chem.*, 1968. **A2**: p. 1441.
- [42] Pan, Y.V., R.A. Wesley, R. Luginbuhl, D.D. Denton, and B.D. Ratner, Plasma polymerized N-Isopropylacrylamide: Synthesis and characterization of a smart thermally responsive coating, *Biomacromolecules*, 2001. **2**: p. 32-36.
- [43] Wang, Y., X. Cheng, Y. Hanein, B. Ratner, and K.F. Böhringer, Protein Patterning with Programmable Surface Chemistry Chips, in *Sixth International Conference on Miniaturized Chemical and Biochemical Analysis Systems (Micro TAS)*. 2002. Nara, Japan.
- [44] Hanein, Y., Y.V. Pan, B.D. Ratner, D.D. Denton, and K.F. Böhringer, Micromachined non-fouling coatings for bio-MEMS applications, *Sensors and Actuators B*, 2001.